Report on kinetics and thermodynamic modelling of radium.

Uptake by barite during recrystallisation experiments at room temperature.

SLOW PROCESSES IN CLOSE-TO-EQUILIBRIUM CONDITIONS FOR RADIONUCLIDES IN WATER/SOLID SYSTEMS OF RELEVANCE TO NUCLEAR WASTE MANAGEMENT

SKIN

DELIVERABLE D4.3

COLLABORATIVE PROJECT (CP)

Grant agreement N°.: FP7-269688

Submitting organizations: PSI
Authors: Enzo Curti
Due date of deliverable: Project Month 34
Actual submission: Project Month 36

Start date of the project: 01 January 2011
Duration: 36 months

Project co-funded by the European Commission under the Seventh Framework Programme of the European Atomic Energy Community (Euratom) for nuclear research and training activities (2007 to 2011)		
Dissemination Level		
PU	Public	×
RE	Restricted to a group specified by the partners of the project	
CO	Confidential, only for partners of the project	

KINETIC AND THERMODYNAMIC MODELLING OF RADIUM UPTAKE BY BARITE DURING RECRYSTALLIZATION EXPERIMENTS AT ROOM TEMEPERATURE

Enzo Curti [1*]

[1]Paul Scherrer Institut, Laboratory for Waste Management (LES), 5232 Villigen PSI (CH)

* Corresponding author: enzo.curti@psi.ch

Summary

This contribution presents the progress made in this task until October 31, 2013. The kinetic/thermodynamic modelling of experimental data produced at FZJ on Ra uptake during the recrystallization of two commercial barites (Sachtleben and Aldrich) was updated and now includes newly supplied data extending up to 658 days reaction time. After a first slow kinetic step, which lasted up to 120-180 days, a sudden decrease towards a minimum aqueous Ra concentration was observed, suggesting fast nucleation from supersaturation of a new $(Ba,Ra)SO_4$ solid solution with ideal or even negative interaction parameter ($a_0 \leq 0$). This step corresponded to growth rates of up to 400 μmol $m^{-2}d^{-1}$. After this fast nucleation step, Ra concentrations in the aqueous solution slowly increased, approaching the equilibrium line of a regular $(Ba,Ra)SO_4$ solid solution with interaction parameter a_0=1.0, in agreement with theoretical predictions based on atomistic simulations. Therefore, these data indicate non-equilibrium Ra entrapment during the mentioned fast precipitation event, followed by slow recrystallization towards true thermodynamic solid solution equilibrium.

The Ra uptake experiments carried out at CHALMERS and KIT-INE involved lower (picomolar to nanomolar) total Ra concentrations, compared to the FZJ experiments (micromolar Ra concentrations). Moreover, in these experiments ^{133}Ba tracer was added simultaneously to the Ra tracer, allowing an independent determination of $(Ra,Ba)SO_4$ growth rates. The Ba tracer data indicate for both sets of experiments recrystallization rates and a_0-values comparable to those inferred from earlier published experiments conducted in a similar range of aqueous Ra concentration. However, the results of the KIT-INE experiments could not be interpreted in terms of the classical *heterogeneous* and *homogeneous recrystallization* models. A new model, requiring repeated dissolution-precipitation of previously formed Ra-

barite monolayers and baptised "*continuous recrystallization* model", successfully described the Ra-uptake experiments conducted at KIT-INE. The different growth mechanism inferred for these experiments may be related to much longer pre-equilibration times of the initial pure barite (seven months, compared to a maximum of few weeks in the other experiments).

Thermodynamic modelling indicates for the CHALMERS data formation of regular $(Ra,Ba)SO_4$ solid solutions with moderately positive interaction parameters (a_0 = 0.7-1.2), whereas the KIT-INE data point to the formation of solid solutions close to ideality.

One of the essential results arising from the three experimental studies is that the non-dimensional interaction parameter describing the formation of the binary $(Ba,Ra)SO_4$ solid solution ranges between a_0 = 0.0 and a_0 ~ 1.0. The latter value seems to reflect long-term thermodynamic equilibrium and agrees with theoretical predictions based on atomistic simulations. This finding has direct relevance for the safety assessment of radioactive waste repository sites, since it constrains the solubility and thus the mobility of radium in such environments.

Background and Objectives

It is well known that a minor element precipitating within a dilute solid solution will have a much lower solubility than if the same element is precipitated as isostructural pure solid. This effect may be particularly beneficial for the safety assessment of radioactive repository sites, if it can be shown that radionuclides released from the waste will form dilute solid solutions with secondary host minerals. In the case of radium, formation of $(Ra,Ba)SO_4$ solid solutions by reaction of sulphate-rich aqueous solutions with Ba and Ra isotopes released via waste corrosion is considered to be likely (Curti et al., 2010; Bosbach et al., 2010). This process would reduce the concentration of dissolved radium in the mobile aqueous phase by orders of magnitude compared to a system in which the solubility is controlled by pure radium sulphate. Eventually, the mobility of ^{226}Ra and its contribution to radiological doses would decrease to levels largely below those predicted assuming that a pure solid (e.g. $RaSO_4$) controls Ra solubility.

A thorough understanding of the mechanisms leading to Ra-barite formation and the careful quantification of related thermodynamic data (non-ideality parameters, end-member solubility products) is a prerequisite to reliably predict the contribution of ^{226}Ra to radiological doses in safety assessment calculations. In this work package, the main objectives were: (1) to model experimental data provided by other SKIN partners on the uptake of Ra during barite recrystallization in terms of solid solution thermodynamics (determination of interaction parameters) and kinetics (growth rates of radiobarites); (2) to review available data on $RaSO_4$ solubility product, in order to verify the reliability of the values currently used in thermodynamic databases.

Recrystallization models

Classical models

In a recrystallization process, also called replacement, a newly formed *secondary* phase grows at the expense of a dissolving *primary* phase ***(Putnis, 2009)***. In this study, the primary phase is pure barite, whereas the secondary phase is Ra-barite solid solution. Barite recrystallization rates can be determined by adding a known aliquot of ^{133}Ba radiotracer to an aqueous suspension of barite particles and then monitoring the gamma activity of the aqueous solution over time. The ^{133}Ba removed from solution is necessarily incorporated in the secondary (growing) phase and is thus indicator of the amount of newly formed barite solid solution. The rate of ^{133}Ba removal is proportional to the growth rate of the secondary barite, which is defined here with the term "recrystallization rate".

Recrystallization rates derived by isotope tracer methods in batch experiments are forcedly model-dependent, since they are associated to conceptual ideas of the recrystallization mechanisms at the microscopic scale. So far, two such idealized mechanisms have been tested (***Curti et al., 2010***): the so-called *homogeneous* and *heterogeneous* incorporation models as described by ***Doerner and Hoskins (1925)*** and ***McIntire (1963)***. These models describe trace element uptake during coprecipitation with a solid precipitated from oversaturated solutions. During homogeneous incorporation, the *total amount* of recrystallized (i.e. newly precipitated) solid is at all times in full equilibrium with the solution, so that the trace element is distributed homogeneously within the growing solid. The trace element concentration in the solid changes with time, but there is no internal concentration gradient.

In the case of heterogeneous incorporation, the equilibrium between growing solid and aqueous solution is limited to a thin surface layer, ideally a few atomic monolayers thick. As recrystallization proceeds, this surface layer is covered by newly precipitated solid and becomes inert, i.e. isolated from exchange with the aqueous solution. In such systems, no full thermodynamic equilibrium is reached, only partial equilibrium between aqueous solution and a thin mineral surface layer exists. Consequently, there is no internal equilibration of the growing crystals and the trace element distribution within the solid will be in general heterogeneous, giving rise to the characteristic concentric zoning patterns frequently observed in natural crystals.

The original homogeneous and heterogeneous models were originally developed for foreign elements coprecipitating with a host solid from an oversaturated aqueous solution (e.g. Sr^{2+} in $CaCO_3$). In ^{133}Ba-barite recrystallization experiments, a tracer isotope of Ba (^{133}Ba) is incorporated in pure $BaSO_4$ under close-to-equilibrium conditions. This required a different mathematical development of the aforementioned models, which is described in ***Curti et al. (2010)***, leading to the following equations:

$$\frac{A_L(t)}{A_S(t)} = \frac{[Ba]}{\nu(t)\,\sigma\,(S/V)+[Ba]} \qquad \text{homogeneous incorporation} \qquad (1)$$

$$\frac{A_L(t)}{A_S(t)} = \exp\left\{\frac{-\nu(t)\,\sigma\,(S/V)}{[Ba]}\right\} \qquad \text{heterogeneous incorporation} \qquad (2)$$

where $A_L(t)/A_S(t)$ is the ratio of ^{133}Ba activity in the aqueous solution sampled from the barite suspension at time t to that of a standard solution containing the total initial ^{133}Ba activity, ν(t) is the amount of barite recrystallized per unit mineral surface area [mol m^{-2}], [Ba] is the total Ba concentration in aqueous solution (M), σ is the specific surface area [m^2 g^{-1}] of the initial barite and (S/V) is the solid to liquid ratio (g l^{-1}). Solving for $\nu(t)$ allows to construct curves of the amount of barite recrystallized versus time. The recrystallization rate R [mol m^{-2} d^{-1}] is then simply the time derivative d$\nu(t)$/dt. Assuming a constant recrystallization rate R, $\nu(t)$ can be replaced by $R\ t$, and the two equations can be used to test the two models against the measured ^{133}Ba activity data, using R as adjustable parameter. Although there is no guarantee that recrystallization will proceed at constant rate, a perfect fit to the activity data using a given model with constant rate would be a strong indication in favor of the recrystallization mechanism assumed in that model. For instance, the recrystallization data of ***Curti et al. (2010)*** could be fitted satisfactorily by applying the homogeneous incorporation model with a constant rate, whereas it was not possible to do the same by applying the heterogeneous recrystallization model.

The "continuous recrystallization" model

In the classical recrystallization models described in the preceding section, it is implicitly assumed that dissolution-reprecipitation is a "one way" process, i.e. the primary phase dissolves and a new, stable phase is produced in a single step. Here, we describe a new model (denoted "*continuous recrystallization* model") in which it is assumed that each infinitesimal layer of newly formed solid undergoes repeated recrystallization cycles during the course of the process. This model was developed after realizing that the data obtained at KIT-INE cannot be explained by the classical models and yielded satisfactory fits to those data (see later).

The continuous recrystallization model assumes monolayer by monolayer recrystallization from outside towards the internal part of the primary crystals, i.e. it follows a pseudomorphic replacement model (see Fig. A1.1, Appendix A1) as described by ***Putnis (2009)***, although it may well be extended to systems where primary and secondary phase are separated in space. A monolayer is a single atomic layer (thickness d = 3.5 x 10^{-10} m for barite). After the first monolayer of the primary pure mineral is dissolved, it reprecipitates in situ as more stable

phase, for instance as Ra-barite solid solution. The solution then reacts with the next monolayer of primary solid and the same recrystallization step takes place, and so on.

The basic idea is that, before a given monolayer of the primary solid is dissolved and re-precipitated, all the previously formed secondary solid must recrystallize again in order to adjust to the new solution composition. This means that all monolayers except the most internal one at the reaction front will have to recrystallize repeatedly. The total amount of mineral recrystallized in such a process (the integral) is at any time larger than the visible (net) amount of recrystallized solid. A more detailed explanation and the mathematical development of the model are given in Appendix 1.

Modelling of FZJ data

Experimental

Extensive Ra uptake experiments were carried out at FZJ. In these experiments, conducted at room temperature (RT) and 90 ^{0}C, two commercial barite powders, Sachtleben® (SL) and Aldrich® (AL) were aged in 0.1 M NaCl + 5 μM $RaBr_2$ solutions during up to 658 days. The Ra concentration in solution was measured by gamma spectrometry at regular intervals. Here, we present modelling work performed on the data delivered until October 31, 2013.

Kinetic model

Because no ^{133}Ba exchange experiments were carried out at FZJ, an identification of the recrystallization mechanisms based on the models described in the previous chapter is not possible. However, it is possible to derive recrystallization rates for homogeneous recrystallization by the fitting procedure described below.

In the basic equation, the recrystallization time t (s) is expressed as a function of the amount of newly formed barite solid solution n (mol), the specific surface area σ (m^2/g), the solution volume V (l), the solid to liquid ratio S/V (g/l) and a surface-normalized recrystallization rate R (mol m^{-2} d^{-1}):

$$t = \frac{n}{\sigma V (S/V) R} \qquad (3)$$

In the equation above, σ is a constant equated to σ_0, the initial mineral surface area. New particle size distribution data, based on SEM images, showed however that the specific surface area of AL barite had decreased by about a factor of two after 443 days ageing in the presence of Ra-bearing solution. A much smaller decrease (less than 10%) was observed for SL barite under the same conditions. In order to evaluate the effect of variations in mineral surface area, the simple growth kinetics model described by eq. 3 has been extended. To implement surface area variations in a simple way, we assumed that the mineral surface area

is varying linearly with the progress of recrystallization between the initial value σ_0 and a final value σ_f:

$$\sigma(n) = \sigma_0 + \frac{n}{n_0}\left(\sigma_f - \sigma_0\right) \quad (4)$$

For the practical implementation, we used quantities scaled to 1 kg of water solvent (~ 1 L), thus the above equation is expressed as:

$$\sigma(n) = \sigma_0 + \frac{[n]}{[n_0]}\left(\sigma_f - \sigma_0\right) \quad (5)$$

where square bracket denote molar concentrations. Introducing the molar weight of barite (MW_{barite}) and noting that $[n_0] = (S/V) / MW_{barite}$ one obtains:

$$\sigma(n) = \sigma_0 + \frac{MW_{barite}[n]}{(S/L)}\left(\sigma_f - \sigma_0\right) \quad (6)$$

Substitution of eq. (6) into eq. (3) yields finally:

$$t = \frac{[n]}{\left[(S/L)\sigma_0 + MW_{barite}[n]\left(\sigma_f - \sigma_0\right)\right] R} \quad (7)$$

Equation (7) can be used to calculate the reaction time needed to grow an amount n of solid solution at a constant growth rate R in a suspension of mass concentration (S/V) while the specific surface area varies linearly between an initial value σ_0 and an endpoint σ_f. The values of n are calculated separately via the GEM-Selektor code ***(Kulik et al., 2013; Wagner et al., 2012)*** for a given solid solution model, characterized by the interaction parameter a_0.

The Ra concentration data were fitted using the following two-step procedure:

(a) Calculation of a series of equilibrium states as a function of the increasing amount (n) of $(Ra,Ba)SO_4$ with the GEM-Selektor (GEMS) code. This yields the equilibrium Ra concentrations as a function of n up to the total amount of barite used in the experiments and for the selected solid solution model (ideal or non-ideal).

(b) Determination of the reaction time $t(n)$ via eq. (7)

For each value of n calculated with GEMS, a reaction time can be computed from the equation above. Because the GEMS calculations include the concentrations of Ra at equilibrium with the selected solid solution, each $t(n)$ value can be readily associated to the corresponding equilibrium Ra concentration, [Ra](n). Since there is no independent determination of the recrystallization rate in these experiments, R was used as adjustable parameter to fit the Ra concentration data.

RT experiments at 0.5 g/l

The data of the two experiments carried out at RT with SL and AL barites at 0.5 g/l are illustrated in Fig. 4.3.1a and 4.3.1b with model curves for ideal solid solutions (blue) and regular solid solution with interaction parameter a_0=1. The latter value corresponds to the theoretical equilibrium value of a_0 recently determined via atomistic simulations by the double defect method (***Vinograd et al., 2013***). Continuous lines correspond to the usual model with constant specific surface area fixed at the initial value, whereas the blue stippled line in Fig. 4.3.1b was calculated assuming a linear reduction of σ to half the initial value (from 1.7 to 0.85 m^2/g).

In both experiments, an initially slow decrease in the aqueous Ra concentration, simulated through a constant recrystallization rate R_1, is followed by a sudden decrease of 1-2 orders of magnitude after about 100 days (SL) or 180 days (AL). Simulating this second kinetic step required much higher rates than for the initial stage ($R_2 >> R_1$). Whereas the growth rates inferred for the first kinetic stage are in the order of magnitude of recrystallization rates determined through ^{133}Ba exchange in previous Ra-barite uptake experiments (***Curti et al. 2010; Bosbach et al., 2010***) the high extrapolated R_2 values are, at least for the tests with SL barite, much faster. They probably indicate sudden nucleation of a new Ra-barite phase. During this step, the Ra concentration in the aqueous phase decreased below the ideal solid solution line, indicating negative values for the interaction parameter a_0. After reaching a minimum at 200 days (SL) and 350 days (AL) the aqueous Ra concentration slowly increases, approaching in both cases (though not reaching) the a_0=1.0 equilibrium lines. At the time of this reporting, no steady state was attained yet, but the observed behaviour strongly suggests that after the fast nucleation step the Ra-barite slowly recrystallizes towards an equilibrium state close to the theoretically predicted a_0 value of 1.0 (***Vinograd et al., 2013***). Therefore, the sudden Ra decrease at 100/180 days probably represents non-equilibrium entrapment (see deliverable D4.2), not a thermodynamic equilibrium state.

Fig. 4.3.1b also shows the effect of decreasing surface area according to eq. 7 (blue stippled line). We recall that in the applied kinetic model recrystallization is assumed to occur epitaxially on the pre-existing mineral surface and is thus proportional to surface area. As expected, reducing the available surface area leads to a delay in attaining equilibrium conditions (the horizontal, constant Ra concentration line). It is quite evident that the predicted effect is opposite to the observed slight increase in Ra concentrations observed at long reaction times. This observation and the very high inferred growth rates (up to 400 μm m^{-2} d^{-1}) suggest that growth rates of the newly formed barites are not proportional to the bulk mineral surface. This conclusion is corroborated by the surprising observation that SL barite is much more reactive than AL barite, although the latter has a 10 times larger specific surface area than SL barite (1.7 m^2g^{-1} vs.0.17 m^2g^{-1}).

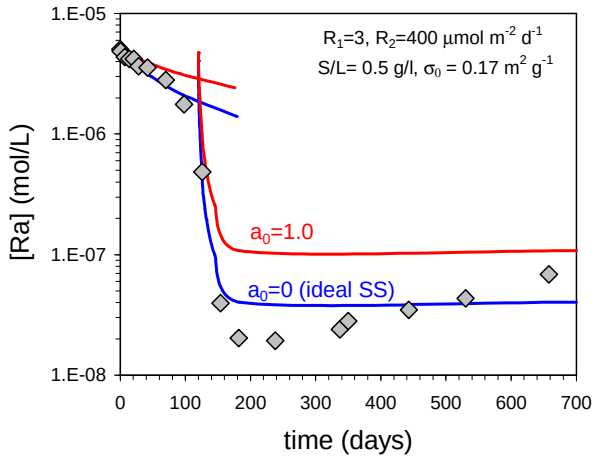

(a) SL barite

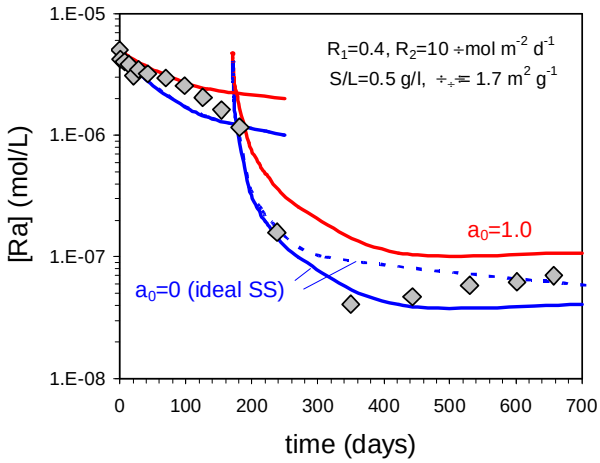

(b) AL barite

Figure 4.3.1: *Experimental data of FZJ Ra-barite recrystallization experiments carried out at room temperature and S/V= 0.5 g/l, compared with model calculations (see text for explanations).*

RT experiments at 5 g/l

The higher reactivity of SL barite is clearly observable also in the experiments conducted at 5 g/l, as shown in Fig. 4.3.2a, where the results of two such experiments are compared to those of the previously discussed 0.5 g/l experiments. In general, the second (fast) kinetic stage of Ra precipitation occurs earlier in the 5 g/l experiments, or is even absent. Moreover, it is evident from Fig. 4.3.2b that the onset of fast Ra uptake occurs at different, unpredictable times, which is also an indication for a sudden nucleation process.

The growth rates inferred for the 5 g/l experiments are reasonably consistent with those derived for the 0.5 g/l experiments. A main difference between the two sets of experiments is the earlier onset of the fast precipitation stage in the 5 g/l tests (less than 30 days).

The a_0 values corresponding to the minima of aqueous Ra concentrations were found to be close to 0 (ideal solid solution) for the 5 g/l tests and even negative for the 0.5 g/l tests. Contrary to the 0.5 g/l experiments, a subsequent slow increase in Ra concentration is barely visible in the 5 g/l tests. This may be related to the fact that a much larger mass of Ra-barite is formed at such high S/L. Consequently, a much longer time is required in order to release and re-precipitate the entrapped Ra in a thermodynamically stable $(Ra,Ba)SO_4$ phase with a_0=1, via recrystallization.

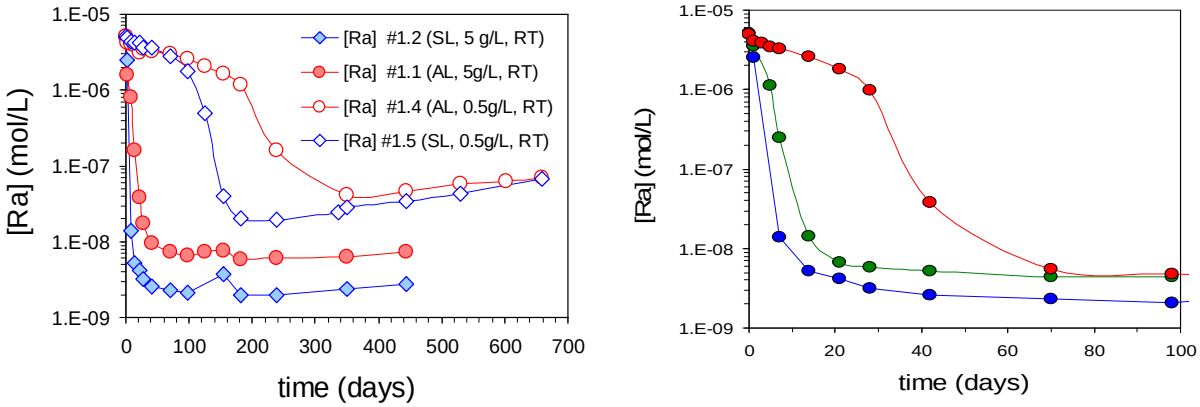

Figure 4.3.2: *(a) Comparison of Ra-barite uptake experiments carried out at FZJ with 0.5 g/l (open symbols) and 5 g/l S/V ratio (full symbols). (b) Three different 5 g/l experiments carried out with SL barite showing different onset times of fast Ra precipitation.*

Effect of thermodynamic data uncertainty

The thermochemical data applied to predict aqueous-solid equilibria in the chemical system of interest (Ra-Ba-Na-S-Cl-O-H at 298 K and 1 bar) are in general of good quality. Some minor uncertainty remains on the solubility product of $RaSO_4$, as described in the 2nd annual workshop proceedings (pp.138-139). All calculations discussed until now have been carried out using the Nagra-PSI database (***Hummel et al., 2002***) which includes a value of -10.26 for log $K_s^0(RaSO_4)$. In order to evaluate the effect of the uncertainty in the solubility product of Ra sulphate, comparative calculations have been carried out using the lowest limit of the uncertainty range, i.e. log $K_s^0(RaSO_4)$ = -10.40. The rationale for selecting the lowest limit was to verify whether the mentioned negative a_0-values would disappear assuming a lower log $K_s^0(RaSO_4)$. Fig. 4.3.3 shows that this is not the case. The effect of decreasing log $K_s^0(RaSO_4)$ from -10.26 to -10.40 is small and insufficient to "avoid" the Ra concentration minima to be below the ideal solid solution line.

In summary, it can be concluded that the interpretation of the chemical processes occurring during the Ra uptake experiments conducted at FZJ does not depend on uncertainties in the solubility product of $RaSO_4$.

Barium concentrations in the aqueous phase

Fig. 4.3.4 shows Ba concentrations measured by ICP-MS for selected Ra-uptake experiments as a function of reaction time. The red lines show the theoretical solubility of Ba in equilibrium with pure barite for the system of interest, i.e. 3.0 x 10^{-5} M in 0.1 M NaCl.

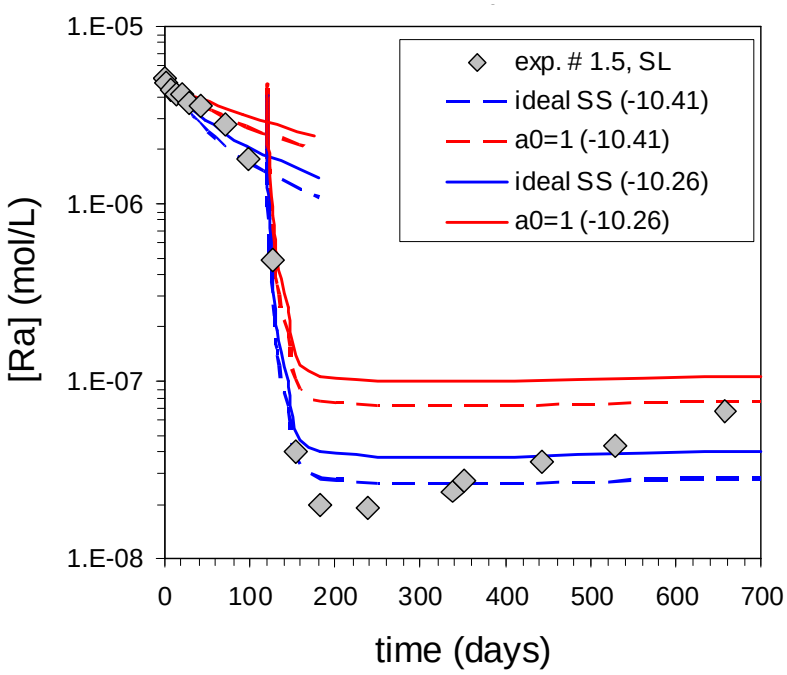

Figure 4.3.3: *Comparative kinetic-thermodynamic model for experiment #1.5, carried out with SL barite at 0.5 g/L. Continuous lines indicate calculations carried out with log $K_s^0(RaSO_4)$ = -10.26; broken lines show the results obtained assuming $K_s^0(RaSO_4)$ = -10.40. Blue curves were obtained assuming formation of ideal $(Ba,Ra)SO_4$ solid solutions, whereas red curves are predictions for regular solid solutions with interaction parameter a_0=1.0.*

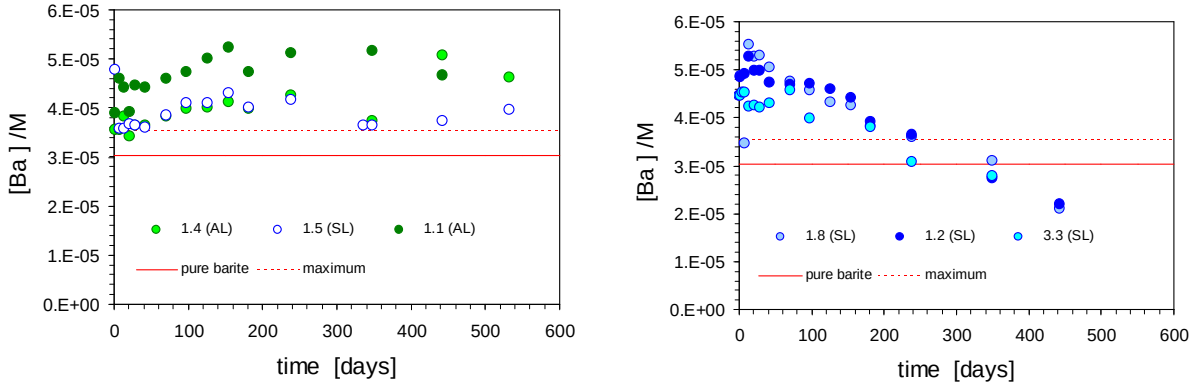

(a) **(b)**

Figure 4.3.4*: Temporal evolution of aqueous Ba concentrations during the Ra-barite experiments carried out at FZJ: (a) 0.5 g/L experiments, (b) 5 g/L experiments. The red continuous line denotes saturation equilibrium with pure barite in the initial solutions. The red dotted line shows the upper limit of Ba concentrations in equilibrium with $(Ba,Ra)SO_4$.*

The plot on the left side (a) refers to the experiments conducted at *S/V*=0.5 g/l. All data points so far measured for these experiments indicate Ba concentrations significantly larger than the theoretical equilibrium concentration in equilibrium with pure barite. When a solid solution forms, the concentration of the host cation in solution should in principle decrease due to the dilution effect caused by the incorporation of foreign ions. A possible reduction in aqueous Ba concentration caused by formation of $(Ba,Ra)SO_4$ solid solution in our system would be however negligible, since the mole fraction of $RaSO_4$ is very small in these $BaSO_4$ dominated systems. On the other hand, incorporation of radium in $(Ba,Ra)SO_4$ via recrystallization of initially pure $BaSO_4$ will displace some Ba to the solution. Assuming a limiting (non-equilibrium) case in which all Ra (5×10^{-6} M) is trapped in the recrystallized solid and an equivalent excess of Ba is released to solution, the upper limit of the final Ba concentration for a constant molar amount of barite present at all times will be $3.0 \times 10^{-5} + 5 \times 10^{-6} = 3.5 \times 10^{-5}$ M. This limit, imposed by mass balance constraints in a closed system, is shown as dotted red line in Fig. 4.3.4. However, practically all 0.5 g/l Ba concentrations and most of the 5 g/l Ba concentrations (up to about 200 days) lie above the dotted red line. This indicates that dissolution initially prevails over precipitation, leading to supersaturation. All data points above the dotted red line represent solutions supersaturated with respect to both pure and Ra-bearing barite. Such behaviour is expected during dissolution-precipitation driven recrystallization and is indeed corroborated by the Ra data in the experiments conducted at 0.5 g/l. The evolution in the 5 g/l experiments is somehow different. After initially quite high degrees of supersaturation, which correlate quite well with the previously discussed early onset of fast Ra precipitation, the Ba concentrations steadily decrease, suggesting that saturation equilibrium is slowly approached. One would expect then Ba concentrations to reach constant (time-independent) values between the two red lines. However, the last two data points at t = 443 days indicate Ba concentrations clearly below the saturation line, which cannot be explained at the moment. Future measurements will have to be awaited in order to decide on the relevance of these two measurements.

Modelling of KIT-INE data

Experimental

Recrystallization experiments have been carried out with SL barite in 0.1 M NaCl at a mass concentration of 0.1 g/l, at room temperature and with ^{133}Ba and ^{226}Ra simultaneously present. The SL barite had been previously aged in aqueous solution during 7 months. The simultaneous use of ^{133}Ba and ^{226}Ra tracers allowed an independent determination of the recrystallization rate, i.e. the determined rate is not a fitted parameter. Four experiments were performed, under the conditions described in Table 4.3.1. The Ra concentrations used for these experiments (0.5- 12 nM) are comparable to those used in earlier published experiments (***Curti et al. 2010; Bosbach et al. 2010***) and much lower than in the experiments performed at FZJ (5 μM).

Table 4.3.1*: Summary of barite recrystallization experiments carried out at KIT-INE in the framework of the SKIN project.*

	$[^{133}Ba]_{total}$ (mol/l)	$[^{226}Ra]_{total}$ (mol/l)	pH
A	2.7×10^{-10}	0	5
B	2.7×10^{-10}	4.7×10^{-10}	3.55
C	2.8×10^{-10}	1.1×10^{-9}	3.15
D	2.7×10^{-10}	1.2×10^{-8}	4.17

Recrystallization Kinetics

As previously stated in the "Recrystallization Models" section, it was not possible to reproduce the ^{133}Ba exchange data obtained at KIT-INE using the equations developed for the *homogeneous* and *heterogeneous* incorporation models. Moreover, the removal rate of ^{133}Ba tracer from solution was much slower than in the experiments of ***Curti et al. (2010)*** and ***Bosbach et al. (2010)***. This called for the development of a new model, based on the assumption of permanent recrystallization of the newly formed secondary barite to adapt for the continuosly changing aqueous phase composition. Accordingly, this model (see Appendix A1 for details) is called here *continuous recrystallization* model.

Figure 4.3.5 shows the modelling results for the four experiments conducted at KIT-INE. In the left column, best fit curves are shown for the three previously discussed recrystallization models, in a plot where the ^{133}Ba activity in solution A_L (normalized to the total added activity measured from standard solution, A_S) is represented as a function of reaction time.

The red curves correspond to the heterogeneous incorporation model, the green curves to the homogeneous incorporation model and finally blue curves depict the behaviour expected if the continuous recrystallization model applies. Whereas for experiments A and B model discrimination is difficult, due to considerable scattering in the data and a limited decrease in tracer concentration, experiments C and D are unequivocally well reproduced only through the continuous recrystallization model. There is no way to reproduce the data assuming either heterogeneous or homogeneous incorporation model with a constant recrystallization rate, as these predict a much faster decrease in ^{133}Ba activity than observed.

The right column in Fig. 4.3.5 shows the *effective* and *bulk* growth rates (R_e and R_b, respectively) corresponding to the continuous recrystallization curves on the left side (i.e. the blue curves). R_e is the rate at which secondary barite is formed at the microscopic scale, assumed to be constant. Because it is assumed that each layer of the barite crystal is being replaced repeatedly, R_e is in general much larger than the macroscopic bulk rate of

replacement, R_b, which refers to the net amount of recrystallized solid and thus decreases with time. Although the effective rate of replacement is very high ($10 < R_e < 173$ μmol m^{-2} d^{-1}) the bulk rate decreases rapidly to values comprised between 1 and 10 μmol m^{-2} d^{-1}, which are quite comparable to the recrystallization rates determined in earlier published experiments, for which either heterogeneous or homogeneous recrystallization mechanisms applied.

Originally, these experiments were carried out with the objective of verifying the influence of Ra on recrystallization kinetics. By comparing Fig. 4.3.5 and Table 4.3.1 one can identify a positive correlation between the added Ra concentration and the rate of removal of ^{133}Ba, suggesting that Ra may catalyze the recrystallization. However, the results correlate even better with the pH-value, which varied from 3.15 to 5 among the four tests. Because it is known that barite dissolution kinetics is pH-dependent (***Dove and Czank, 1995***), the two effects cannot be separated. Further experiments at fixed pH would be required to verify the effect of Ra concentration on barite recrystallization kinetics.

In summary, the model calculations clearly indicate that the "continuous recrystallization" mechanism is more appropriate than the "classical recrystallization models" to explain the results obtained at KIT-INE. There is no doubt that another mechanism is operating in this case, although the reasons are not well understood at the moment. The only systematic difference between these experiments and all other experiments, including those described by ***Curti et al. (2010)*** and ***Bosbach et al. (2010),*** seems to be the longer pre-equilibration time. The SL barite used in the KIT-INE experiments was equilibrated during seven months, whereas ageing time in all other experiments were in the range of hours to weeks.

A further indication that pre-equilibration could play a role in affecting the mechanisms of recrystallization is the fact that the surface area of SL barite decreased from about 0.4 to 0.15 m^2 g^{-1} during the ageing (Heberling, pers. comm.). Another distinctive feature is the simultaneous use of ^{133}Ba and ^{226}Ra tracers in the KIT-INE experiments. However, the presence of Ra cannot be invoked as being the cause of the change in recrystallization mechanism, since Ra was present in experiments B, C and D, but not in experiment A, which was carried out with ^{133}Ba only (as in the mentioned published studies).

Clearly, any further progress in this subject will depend on the ability of using in-situ microscopic methods to unravel the operating dissolution-precipitation mechanisms. Modelling of such batch experiments will not be sufficient to resolve this issue.

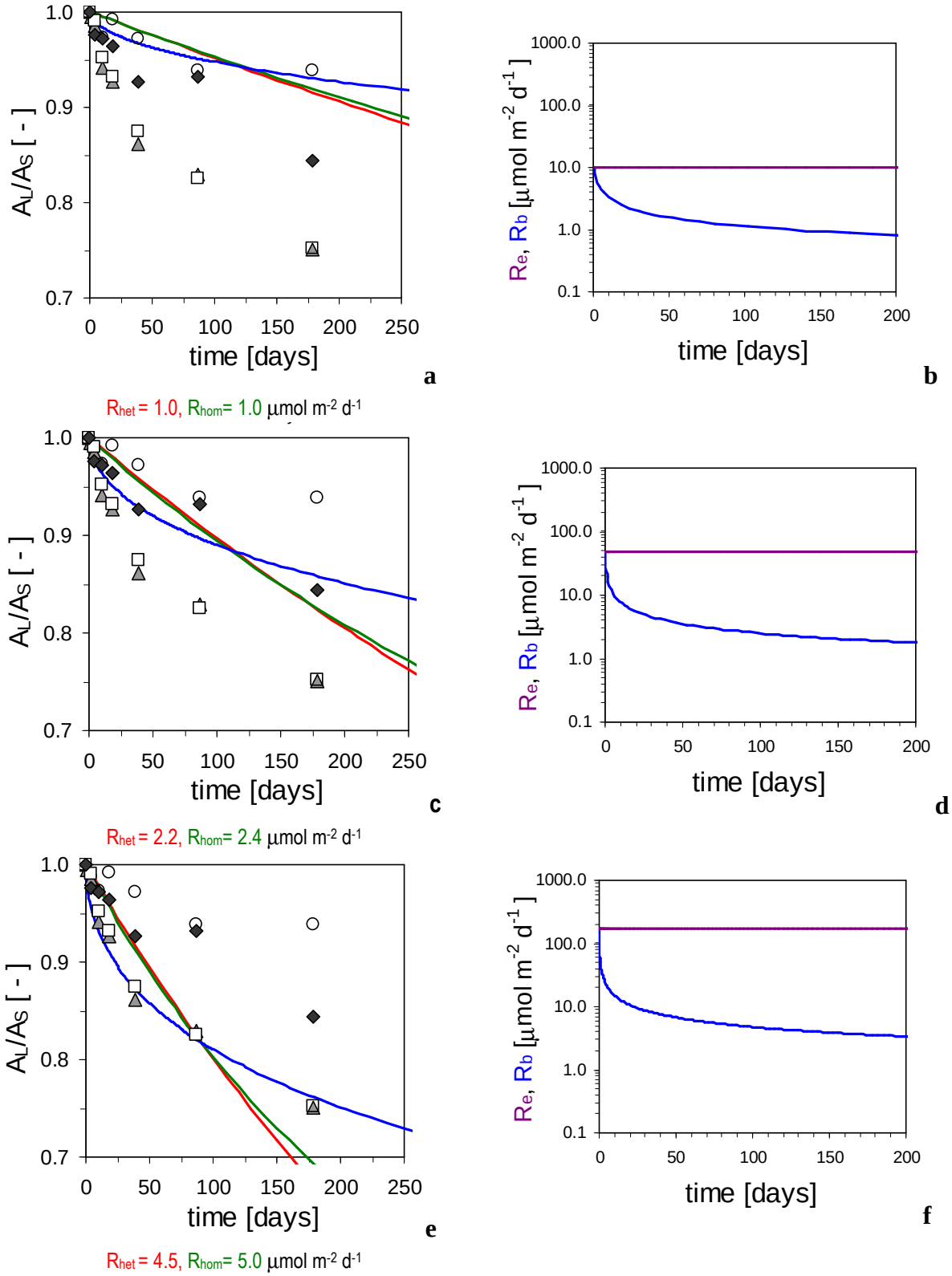

***Figure 4.3.5**: From top to bottom, modelling results for KIT-INE recrystallization data for experiments A (circles), B(rhombs), C(squares) and D (triangles) . See text for explanations.*

Thermodynamic Modelling

We used the combined ^{133}Ba and ^{226}Ra data to model the formation of secondary (Ra,Ba)SO_4 for experiments B, C and D with the help of GEM-Selektor code (http://gems.web.psi.ch). Values of [*n*] (moles of barite recrystallized per liter of solution) were calculated directly from experimental ^{133}Ba(solution)/^{133}Ba(total) ratios (A_L/A_S) and are time independent. For a given value of (A_L/A_S) both homogeneous and continuous recrystallization models yield identical values. It is not possible to correlate the results of our thermodynamic calculations to the heterogeneous recrystallization model, since this is a partial equilibrium model, i.e. the internal parts of the crystals are declared as not being in equilibrium with the solutions. Although tools are now being developed to deal with such non-equilibrium systems (see Kulik and Thien, deliverable D4.2), this work is in progress and beyond the scope of the present study. Fig. 4.3.6 summarizes the results of the calculations in a single plot showing the measured aqueous Ra concentrations as a function of the amount of recrystallized barite. The data are compared to GEMS calculations where formation of either ideal (thick continuous curves) or regular solid solutions with interaction parameters a_0 = +1.0 (dotted curves) and a_0 = -1.0 (broken curves) were assumed. The results point to formation of (Ra,Ba)SO_4 solid solutions close to ideality in all three experiments, independently of the added Ra concentrations. This result contrasts with the updated results from the FZJ experiments, which indicate regular solutions with moderately positive interaction parameter in the long-term ($a_0 \rightarrow 1$ for t > 200 days). Note however that the modelled KIT-INE experiments reach only a reaction time of 179 days.

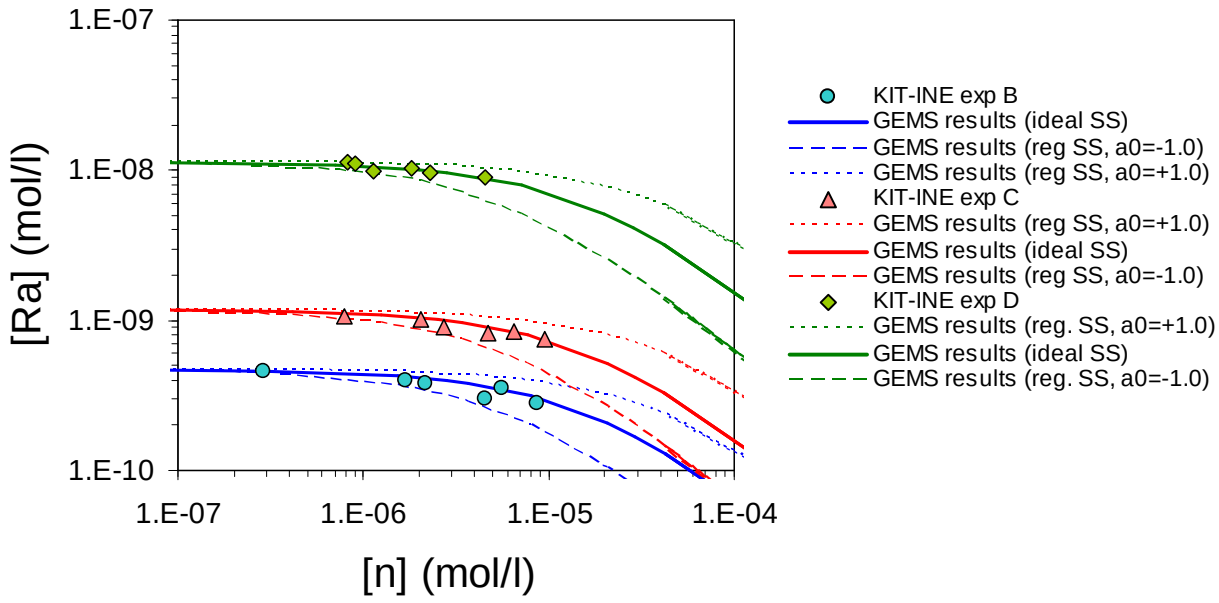

***Figure 4.3.6**: Experimental data from Ra-barite interaction experiments carried out at KIT-INE compared to predicted Ra equilibrium concentrations for ideal and regular solid solution models as a function of the amount of recrystallized barite.*

Modelling of CHALMERS data

Experimental

Ra uptake experiments on self-produced barite were carried out at room temperature with simultaneous addition of ^{223}Ra and ^{133}Ba tracers to monitor the recrystallization kinetics. Three solutions (System 1, 2, 3) containing 100 ml of 0.01 M Na_2SO_4 and 0.05 g of $BaSO_4$ were prepared in 250 ml plastic bottles and pre-equilibrated during 10 days. Thereafter, ^{223}Ra and ^{133}Ba spikes were added. In System 3, only ^{133}Ba was added (Ra-free experiment). The pH of the final suspensions was 5.4. Blank tests without addition of barite showed that no tracer adsorption on the walls of the vessels took place.

Recrystallization Kinetics

Surface normalized rates based on ^{133}Ba data cannot be modeled precisely because the specific surface area of the $BaSO_4$ solid was not determined experimentally. Based on the information that the synthesized $BaSO_4$ was passed through 0.5-1.0 mm sieves and assuming a "roughness factor" of two, a value of σ_0 = 0.0036 m^2 g^{-1} was estimated. The "roughness factor" was determined from available BET surface area and particle size data of other barite powders.

Fig. 4.3.7 shows the best fits for two experiments against the previously discussed homogeneous and heterogeneous recrystallization models, obtained using the aforementioned σ_0 value. The continuous recrystallization model was found to be inappropriate and is therefore not shown.

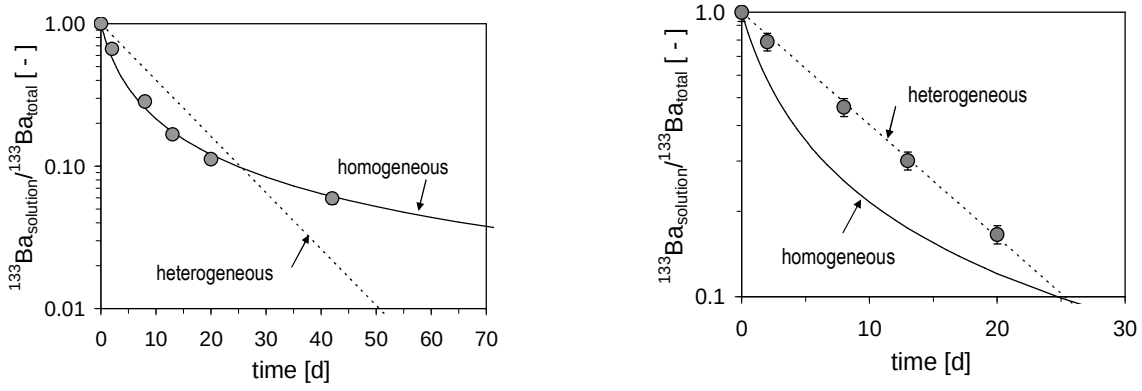

(a) (b)

Figure 4.3.7: *Best fits of ^{133}Ba data from two $BaSO_4$-tracers interaction experiments in 0.01 M Na_2SO_4: (a) System 1 = test with simultaneous addition of ^{223}Ra and ^{133}Ba tracers (only data before addition of a second ^{223}Ra aliquot are considered); (b) System 3 = Ra-free test with addition of ^{133}Ba only.*

In spite of the large uncertainties in recrystallization rates introduced by the approximate value of the barite specific surface area, the current modeling results can nevertheless be used to identify the appropriate recrystallization mechanism. As clearly shown in Fig. 4.3.7a, the data obtained from the System 1 experiment can only be reproduced by the homogeneous recrystallization model. It is not possible to obtain a satisfactory fit with the heterogeneous model, which requires an exponential decrease of the ^{133}Ba activity in solution (*i.e.* a linear decrease in the semi-logarithmic plots of Fig. 4.3.7). Conversely, the data of system 3 define a linear trend, following the heterogeneous recrystallization model.

We have currently no explanation why in the two experiments two different recrystallization mechanisms should operate; we can only suggest that this difference may be related to the presence (System 1) or absence (System 3) of radium in solution. Note that the estimated recrystallization rates of 60 µmol m^{-2} d^{-1} and 15 µmol m^{-2} d^{-1} derived from the best fits of System 1 and System 3 data, respectively, are close to the upper limit of values derived in the experiments of ***Curti et al.(2010)*** and ***Bosbach et al. (2010)***.

System 1 was a double spiking test, *i.e.* a second aliquot of ^{223}Ra was added 42 days after the start of the experiment. At that time, more than 90% of the initial ^{223}Ra had already decayed. Fig. 4.3.8 shows simultaneously the ^{133}Ba and ^{223}Ra aqueous concentration data for this experiment. After the addition of the second ^{223}Ra spike at 42 days, the ^{133}Ba concentration temporarily increased until 45 days (although no second aliquot of ^{133}Ba spike was added), before it then continued to decrease. The close-up of the 40 - 60 days interval (Fig. 4.3.8b) shows clearly that ^{133}Ba starts to increase exactly at the time of the second ^{223}Ra addition.

This short-term, transitory increase in ^{133}Ba is an indication that the Ra-barite formed after the first tracer addition was at least partially dissolved soon after addition of the second ^{223}Ra aliquot. Because most of the ^{223}Ra from the first spike had already decayed at that time (and therefore the secondary Ra-barite had "reverted" to almost pure $BaSO_4$) the addition of a second radium aliquot must have caused a destabilization and thus dissolution of the first (now almost radium free) solid, causing a net release of ^{133}Ba to the aqueous phase. The decrease in ^{223}Ra concentration between 42 and 45 d indicates simultaneous growth of a new secondary Ra-barite. The fact that we can observe a transitory increase in ^{133}Ba implies that the net rate of ^{133}Ba release from the first secondary barite exceeded the rate of ^{133}Ba uptake by the new solid, a quite fortuitous and lucky circumstance revealing the details of the growth and dissolution reactions taking place in this system.

Thermodynamic Modelling

The data obtained at CHALMERS for the System 1 experiment could not be modelled in the same way as the KIT-INE data and the experiments of ***Curti et al. (2010)*** since the Ra uptake was monitored using the short-lived ^{223}Ra tracer ($t_{1/2}$ = 11.3 days) instead of the long-lived ^{226}Ra ($t_{1/2}$ = 1600 years). Using ^{223}Ra has the advantage of decreasing the detection limit far below the picomolar level and avoids generating long-lived radioactive waste. The cost,

however, is that solid solution equilibria will rapidly shift during the laboratory experiments because of fast decay, which is at a comparable timescale as barite growth rates. Because ^{223}Ra decays completely to ^{207}Pb within a few months, the Ra concentrations in a $(Ra,Ba)SO_4$ solid solution will decrease significantly during experiments with duration of up to 60 days.

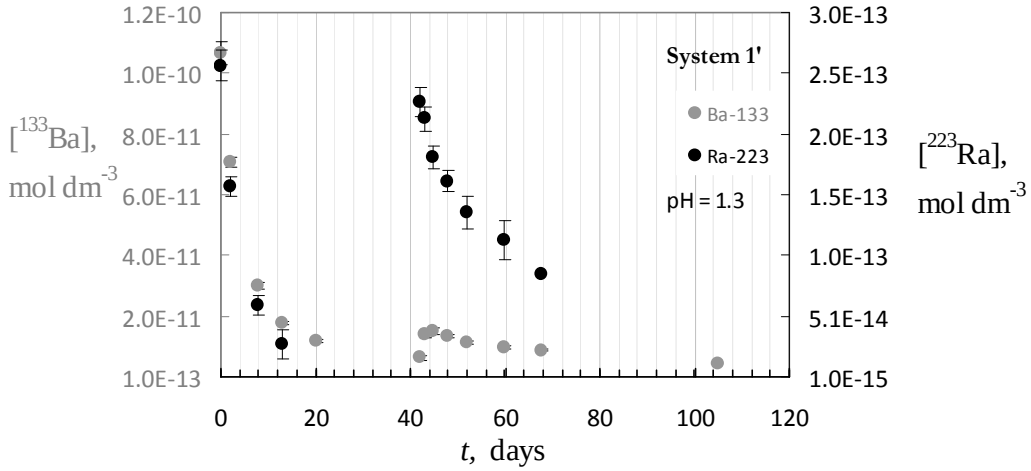

a

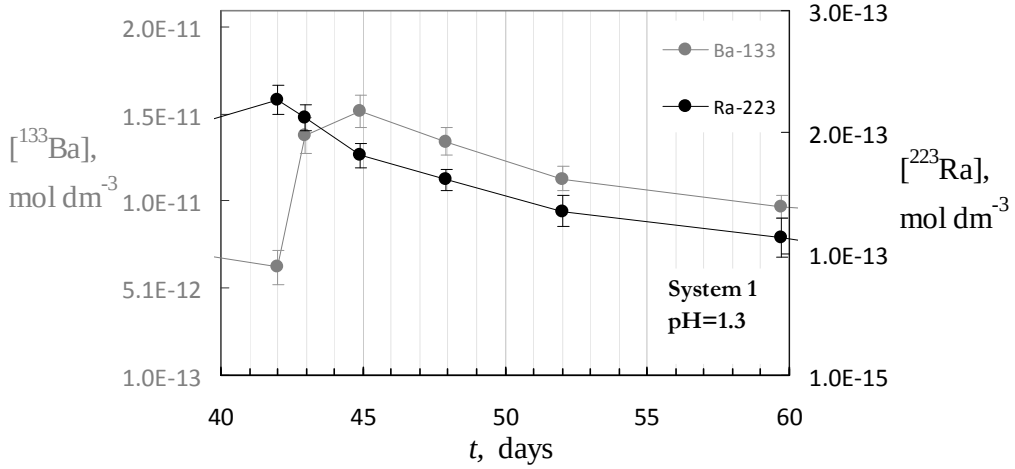

b

Figure 4.3.8*: ^{133}Ba and ^{223}Ra concentrations as a function of reaction time for System 1 experiment: (a) entire experiment; (b) close-up of the time interval shortly before and after the second ^{223}Ra spike addition at t=42 days.*

From the technical point of view, the CHALMERS experiments cannot be modelled exactly in the same way as done for systems doped with ^{226}Ra, because the amount of total Ra in the system is not constant on the time scale of laboratory experiments. Therefore, GEMS calculations were not be carried out with the usual iterative "process" producing model curves as shown in Fig. 4.3.6. A "point by point" strategy was used, by which a separate calculation was carried out for each single data point, taking into account the decay of ^{223}Ra at each sampling time. Moreover, because after addition of the second ^{223}Ra aliquot it is no longer possible to determine [*n*] quantitatively (due to release of ^{133}Ba from the dissolving first recrystallized phase), solid solution thermodynamic calculations had to be restricted to the data before 42 days. This limits our modelling capability to the three data points of System 1 at t = 2, 8 and 13 days.

A short account of the essential input parameters and key results of the GEMS calculations is given in Table 4.3.2. In order to define the initial system, saturation equilibrium was first calculated for pure barite in 0.01 M Na_2SO_4 at the appropriate pH (adjusted by "adding" HCl). This yields the background Ba concentration at the start of the experiment, $[BaSO_4]_{sat}$. The amount of pure barite recrystallized at the given time, $[n]_{inp}$, calculated from the best fit of ^{133}Ba data, was then added to $[BaSO_4]_{sat}$, yielding the total concentration of $BaSO_4$ that has to be specified in the GEMS calculations, $[BaSO_4]_{inp}$.

Table 4.3.2: *Main input (green) and output (blue) of the three GEMS calculations carried out to model (Ra,Ba)SO_4 solid solution formation during System 1 experiment. Each row corresponds to a single experimental point (sampling times at 2, 8 and 13 days).*

GEMS-ID	$[BaSO_4]_{sat}$	$[n]_{inp}$	$[BaSO_4]_{inp}$	$[RaCl_2]_{inp}$	$[n]_{out}$	[Ra]	X(Ra)	a_0
	mol/kgw	mol/kgw	mol/kgw	mol/kgw	mol/kgw	mol/kgw	[-]	[-]
CHALM-1-2d	2.96E-07	1.49E-07	4.45E-07	2.28E-13	1.50E-07	1.58E-13	4.67E-07	0.71
CHALM-1-8d	2.96E-07	7.48E-07	1.04E-06	1.58E-13	7.44E-07	5.96E-14	1.32E-07	1.14
CHALM-1-13d	2.96E-07	1.48E-06	1.77E-06	1.17E-13	1.47E-06	2.78E-14	6.05E-08	1.21

GEMS then calculates the aqueous speciation in thermodynamic equilibrium with the most stable solid(s), which is in our case a (Ra,Ba)SO_4 solid solution. The properties of the solid solution must be specified by selecting appropriate interaction parameters. In our model, we selected a regular solid solution model requiring a single interaction parameter, which is sufficient for dilute binary solid solutions of this kind (Henry's law region). In our calculations, the interaction parameter (W_G [J/mol] or $a_0=W_G/RT$) was varied until the output Ra concentration in aqueous solution matched the experimental values. The results of this fitting procedure, shown in the right-most column of Table 1, indicate consistently positive

interaction parameters. These values are close to the theoretical a_0 (+1.0) calculated by ***Vinograd et al. (2013)*** and to the long-term values approached in the FZJ experiments. They are also close to the lower limit of the a_0-range inferred in the experiments of ***Curti et al. (2010)*** (1.5-2.5). These values however differ from the KIT-INE results, which point to solid solutions close to ideality.

Appendix A1 – Development of the "continuous recrystallization" model

1. Model development

The model postulates that the reacting mineral consists of N equally sized cubic particles with edge length a_0 [m] (Fig. A1.1):

$$N = \frac{(S/L)_0 \, L}{\rho \, a_0^3} \qquad \text{(A1.1)}$$

In the equation above $(S/L)_0$ is the initial solid to liquid ratio [kg m^{-3}], L is the volume of aqueous solution [m^3], ρ is the mineral density [kg m^{-3}].

The basic idea is that, before a given monolayer of the primary solid is dissolved and re-precipitated, the whole previously formed secondary solid must recrystallize again in order to adjust to the new solution composition. This means that all monolayers (except the "last" one at the core of the particle) will have to recrystallize repeatedly. In other words the total amount of mineral recrystallized (the integral) is at any time larger than the net amount of recrystallized solid.

For instance, recrystallization of the layer with index k=2 implies that the first layer must recrystallize a second time, and the layer with index k=3 can recrystallize only after the k=1 layer recrystallizes a third time and the k=2 layer a second time. Therefore, the recrystallization of k mineral layers requires the following effective amount of reprecipitation:

$$n(k) = \frac{N\rho}{W}\left[a_0^3 - (a_0 - 2kd)^3 \right] \qquad \text{(A1.2)}$$

Assuming a constant effective recrystallization rate R_e [mol m^{-2} s^{-1}] it is then possible to calculate the time required for the net recrystallization of k-layers

$$t(k) = \Delta t\,(1 + 2 + 3 + ... k) \qquad => \qquad t(k) = t(k\text{-}1) + k\,\Delta t \qquad \text{(A1.3)}$$

where

$$\Delta t \cong \frac{a_0^3 - (a_0 - 2d)^3}{R_e \, W \, \sigma_0 \, a_0^3} \qquad \text{(A1.4)}$$

where W is the molar weight of barite [g mol^{-1}]. Equation A1.4 is valid when the total amount recrystallized is small (a few % max.) compared to the total amount of primary mineral. This approximation is in general good on the time scale of laboratory experiments and allows one to treat Δt as a constant, which greatly facilitates the derivation of an explicit solution of the model (see later).

It is convenient here to make a clear distinction between the "effective" (R_e) and the "bulk" (R_b) recrystallization rates. R_e represents the rate at which the mineral is dissolved and

reprecipitated at the microscopic (monolayer) scale, whereas R_b corresponds to the macroscopic kinetics, i.e. the net amount of mineral recrystallized per unit time and surface area at any given reaction time t. Defining S_0 as the initial total surface area, one obtains:

$$R_e \equiv \frac{n_{k=1}}{\Delta t\, S_0} = \frac{a_0^3 - (a-2d)^3}{\Delta t\, W\, \sigma_0\, a_0^3} \qquad \text{(A1.5)}$$

$$R_b \equiv \frac{n(k)}{t(k)\, S_0} = \frac{a_0^3 - (a-2kd)^3}{t(k)\, W\, \sigma_0\, a_0^3} \qquad \text{(A1.6)}$$

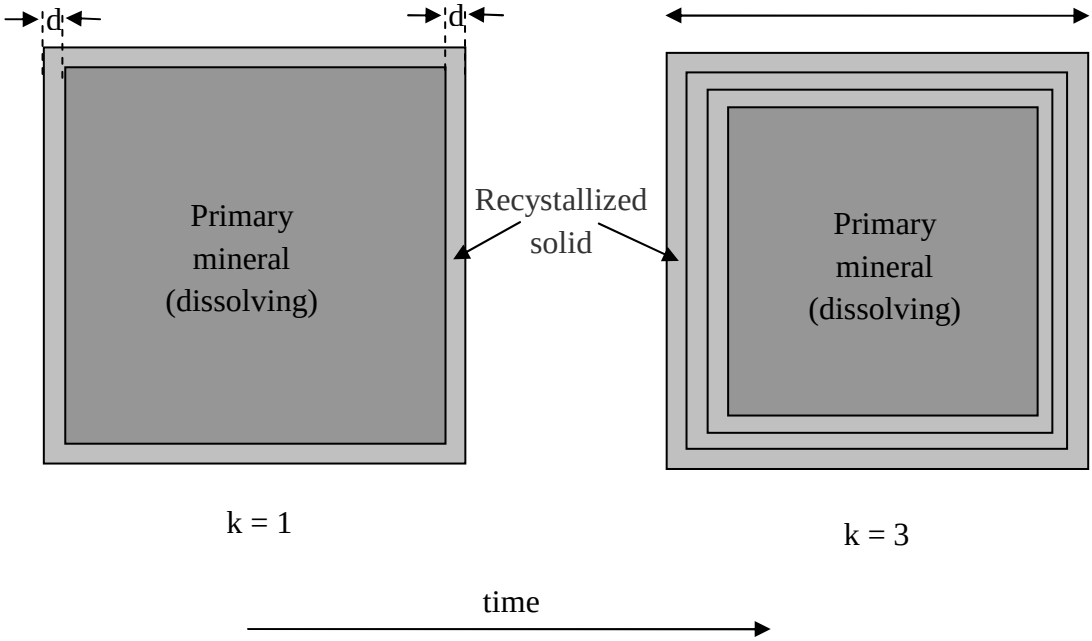

***Fig. A1.1** : Sketch of the proposed recrystallization model, showing the state of a particle after recrystallization of 1 and 3 monolayers, respectively. Parameters and symbols are defined in the text.*

Note that while R_e is a model constant, R_b is a function of k and thus varies (decreases) with time. R_e and R_b are normalized to the *initial* surface area of the dissolving mineral. This is physically not entirely correct, for the following two reasons:

(1) The model assumes that the effective dissolution rate of a monolayer per unit exposed surface area is constant, however for large values of t, $S(t) << S_0$, so $R_b(t)$ should be corrected for the decrease in surface to maintain a physical meaning.

(2) R_e is in principle constant with time, if we regard this quantity as a constant rate of destruction of chemical bonds. Under this premise, at large reaction progress geometrical effects will tend to increase the R_e value, due to the fact that when the particles become very small, the ratio of monolayer volume to particle surface increases.

Alternatively, analogous rates (R^*_e , R^*_b [mol l^{-1} s^{-1}]) can be defined relative to the solution volume. Such rates are insensitive to changes in surface area, but we preferred to stick to the usual surface normalization model to facilitate comparison with data from other experiments.

2. Recursive and explicit forms of the model

The recursive model yields following expressions for the amount of recrystallized barite and time as a function of the index *k*:

$$n(k) = \frac{N\rho}{W}\left[a_0^3 - \left(a_0 - 2kd\right)^3 \right] \qquad \text{(A1.7)}$$

$$t(k) = \frac{k}{2}\left(k+1\right)\Delta t \qquad \text{(A1.8)}$$

Equation A1.7 yields the total number of moles of newly grown barite after *k* monolayers of barite have recrystallized. In equation A1.8, Δt is the time of recrystallization of a single monolayer. Equation A1.8 is the explicit form of the recursion series representing the recrystallization process (eq. A1.3), i.e. $t(k) = \Delta t\ (1 + 2 + 3 + ...+k)$ which is an arithmetic series of the type

$$S_k = d\sum_{i=1}^{k} a_i \quad \text{with general solution } S_k = \frac{k}{2}\left[2a_1 + \left(k-1\right)d \right] \qquad \text{(A1.9)}$$

The series of interest is the particular solution of eq. A1.9 for $a_1 = 1$ and $d = 1$. The time Δt is related to the surface normalized effective recrystallization rate, R_e, by:

$$R_e \cong \frac{n_{k=1}}{\Delta t\ \sigma_0 \left(S/L\right)_0 L} \quad \Rightarrow \quad \Delta t \cong \frac{n_{k=1}}{R_e\ \sigma_0 \left(S/L\right)_0 L} \qquad \text{(A1.10)}$$

One should remember that there is no difference between bulk and effective recrystallization rate for the first monolayer, therefore we can write $n_{k=1}$ in the numerator. Note also that an approximation equality sign was introduced. The exact equation would require to use $\sigma(t)$ and $(S/L)(t)$, but since this would make it impossible to derive an analytical explicit solution for $n(t)$, we were forced to introduce this approximation. The approximation is however good for the present laboratory-scale experiments, where only a minor fraction of the initial barite was dissolved.

Equation A1.10 can be further developed by substituting explicit expressions for $n_{k=1}$ and N, the total number of particles:

$$\Delta t = \frac{a_0^3 - (a - 2d)^3}{R_e W \sigma_0 a_0^3} \tag{A1.11}$$

Now it is evident that Δt can be treated as a constant with adjustable parameter R_e. That is R_e must then be found by fitting the experimental data. After solving eqs. A1.7 and A1.8 for k the following equation is obtained:

$$\frac{a_0 - \left(a_0^3 - \frac{n}{K}\right)^{1/3}}{2d} = \frac{\sqrt{\Delta t^2 + 8\,\Delta t \cdot t}}{2\,\Delta t} - \frac{1}{2} \tag{A1.12}$$

from which the explicit analytical solution for $n(t)$ is derived:

$$n(t) = K\left\{a_0^3 - \left[a_0 + d\left(1 - \frac{\sqrt{\Delta t^2 + 8\Delta t \cdot t}}{\Delta t}\right)\right]^3\right\} \tag{A1.13}$$

where

$$K \equiv \frac{\rho N}{W} = \frac{(S/L)_0 L}{W a_0^3} \tag{A1.14}$$

$$\Delta t = \frac{a_0^3 - (a - 2d)^3}{R_e W \sigma_0 a_0^3} \tag{A1.15}$$

The explicit solution has following advantages compared to the recursive form:

- R_e can be fitted directly in a spreadsheet. The recursive method requires to first fit Δt; R_e can be calculated only after this step.

- A small number of points is sufficient to generate curves for long time spans. The recursive method requires hundreds or thousands of intervals.

Acknowledgement

The research leading to these results has received funding from the European Union's European Atomic Energy Community's (Euratom) Seventh Framework Program FP7-Fission-2010 under grant agreement number 269688 (CP-SKIN). Many thanks are due to the partners FZJ, KIT-INE and CHALMERS, who provided the data and information necessary for the modelling work.

References

Bosbach D., Boettle M. and Metz V. (2010) Experimental study on Ra^{2+} uptake by barite $BaSO_4$. Kinetics of solid solution formation via $BaSO_4$ dissolution and $Ra_xBa_{1-x}SO_4$ (re) precipitation. Technical Report TR-10-4. Svensk Kårnbränslehantering AB. Swedish Nuclear Fuel and Waste Management Company, Stockholm, Sweden.

Curti, E., Fujiwara K., Iijima K., Tits J. Cuesta C., Kitamura A., Glaus M.A. and Müller W. (2010). Radium uptake during barite recrystallization as a function of solution composition at 23 ± ^{o}C: An experimental ^{133}Ba and ^{226}Ra tracer study. Geochim. Cosmochim. Acta **74,** 3553-3570.

Doerner, H.A. and W.M. Hoskins (1925) Co-precipitation of radium and barium sulfates. Journal of the American Chemical Society **47**, 662-675.

Dove P.M. and Czank (1995) Crystal chemical controls on the dissolution kinetics of the isostructural sulfates: Celestite, anglesite, and barite. Geochimica et Cosmochimica Acta **59**, 1907- 1915.

Hummel, W., Berner, U., Curti, E., Pearson, F. J., and Thoenen, T. (2002). Nagra/PSI Chemical Thermodynamic Data Base 01/01. Nagra Technical Report NTB 02-16, Nagra, Wettingen, Switzerland; and Universal Publishers/uPublish.com, Parkland, Florida, ISBN 1-58112-620-4.

Kulik D.A., Wagner T., Dmytrieva S.V., Kosakowski G., Hingerl F.F., Chudnenko K.V., and Berner U. (2013). GEM-Selektor geochemical modeling package: revised algorithm and GEMS3K numerical kernel for coupled simulation codes. Computational Geosciences **17**, 1-24.

McIntire W. L. (1963) Trace element partition coefficients - A review and application to geology. Geochim. Cosmochim. Acta 27, 1209-1264.

Putnis, A. (2009) Mineral Replacement Reactions. In: Reviews in Mineralogy & Geochemistry, Vol. 70, pp. 87-124, Mineralogical Society of America.

Vinograd V.L., Brandt F., Rozov K., Klinkenberg M., Refson K., Winkler B. and Bosbach D. (2013) Solid–aqueous equilibrium in the $BaSO_4$-$RaSO_4$-H_2O system: First-principles calculations and a thermodynamic assessment. Geochim. Cosmochim. Acta **122,** 398–417.

Wagner T., Kulik D.A., Hingerl F.F., and Dmytrieva S.V. (2012). GEM-Selektor geochemical modeling package: TSolMod library and data interface for multicomponent phase models. Canadian Mineralogist **50**, 1173-1195.